Bulletin of Electrical Engineering and Informatics
Vol. 15, No. 6, December 2026, pp. 5173~5190
ISSN: 2302-9285, DOI: 10.11591/eei.v15i6.13199

Machine learning–driven prediction of in vitro dissolution profiles for glipizide solid dispersions

Ali Olamat[1], Hamza Abu Owida[1], Areen Arabiat[2], Pinar Ozel[3]
[1]Department of Medical Engineering, Faculty of Engineering, Al-Ahliyya Amman University, Amman, Jordan
[2]Department of Communications and Computer Engineering, Faculty of Engineering, Al-Ahliyya Amman University, Amman, Jordan
[3]Department of Software Development, Faculty of Computer and Information Technologies, Cappadocia University, Nevşehir, Turkey

Article Info

Article history:

Received Apr 26, 2026
Revised Sep 4, 2026
Accepted Sep 12, 2026

Keywords:

Dissolution profile
Glipizide
Machine learning
Predictive modeling
Solid dispersion

ABSTRACT

In vitro dissolution profiling is central to developing oral dosage forms of poorly water-soluble drugs. Glipizide shows solubility-limited performance, so polymer-based solid dispersions (SDs) (polyvinylpyrrolidone (PVP) K30, PVP K90, polyethylene glycols (PEG) 6000) are used to enhance dissolution. Using percent-release profiles digitized from a published source, dissolution trajectories from 16 formulations—spanning multiple drug: polymer ratios plus reference tablets—were modeled from long-format time-series. Features comprised formulation metadata, engineered time descriptors, and optional kinetic-fit descriptors. Five approaches—bagged trees, least squares boosting (LSBoost), support vector regression (SVR), Gaussian process regression (GPR), and a long short-term memory (LSTM) sequence-to-sequence model—were compared using grouped 5-fold cross-validation by formulation to prevent time-point leakage, with performance assessed by root mean square error (RMSE), mean absolute error (MAE), and coefficient of determination (R^2). Bagged trees (RMSE 18.90%; R^2 0.701) and the LSTM (RMSE 19.18%; R^2 0.692) performed best and were statistically indistinguishable, while LSBoost was moderate and SVR and GPR underfit, producing near-constant predictions and negative R^2. Curve overlays showed the leading models preserved polymer-family separation and key dissolution-shape features, with occasional formulation-level outliers under strict holdout. Under formulation-level generalization, tree ensembles and sequence models predict glipizide SD dissolution with useful accuracy, supporting more efficient screening and rational optimization.

This is an open access article under the CC BY-SA license.

Corresponding Author:

Areen Arabiat
Department of Communications and Computer Engineering, Faculty of Engineering
Al-Ahliyya Amman University
Al-Salt, Amman, Jordan
Email: a.arabiat@ammanu.edu.jo

1. INTRODUCTION

In vitro dissolution profiling refers to the quantitative measurement of the rate and extent of drug release from a dosage form into a dissolution medium under standardized conditions. Beyond being a routine quality-control test, dissolution is central to pharmaceutical sciences because it links formulation and manufacturing variables to in vivo performance, particularly for oral drug delivery systems in which release and solubilization can be rate-limiting steps for absorption [1]. Historically, dissolution science evolved from foundational transport concepts such as concentration-gradient–driven dissolution into a regulatory and biopharmaceutic cornerstone supporting formulation optimization, post-approval changes, and, under defined

conditions, biowaivers based on the biopharmaceutics classification system (BCS) [2]. Its regulatory importance is reflected in general pharmacopeial chapters that standardize apparatus, media, agitation, sampling, and acceptance criteria, and in international guidance on setting specifications and justifying test procedures for new drug products [3].

Traditional evaluation of dissolution profiles relies on single-point specifications (e.g., % dissolved at a specified time), model-independent comparisons such as difference and similarity factors, and model-dependent kinetic fitting (e.g., Weibull or other empirical/semi-mechanistic functions). These approaches have been widely used to compare multi-sampling dissolution curves, particularly in bioequivalence and formulation-comparability settings, provided that assumptions on sampling times and variability are satisfied [4], [5]. While indispensable, they can become limiting when dissolution behavior is shaped by high-dimensional interactions among drug properties, excipient selection, microstructure, and processing conditions, and when mechanistic assumptions (constant surface area, sink conditions, and simplified geometry) do not hold for modern delivery systems [6], [7]. Consequently, there is growing interest in data-driven strategies that learn complex relationships from experimental datasets.

Solid dispersions (SDs) are multicomponent solid-state systems in which an active pharmaceutical ingredient (API) is dispersed within an inert carrier or matrix often a hydrophilic polymer at the molecular, amorphous, or microcrystalline level. They originated from early eutectic-mixture concepts aimed at improving dissolution and absorption of poorly soluble drugs [8] and were later formalized into broader pharmaceutical applications spanning crystalline dispersions, amorphous solid solutions, and polymer-based glass solutions [9]. SDs enhance apparent solubility and dissolution performance through multiple, often concurrent mechanisms: reduction of effective particle size to the molecular scale, improved wettability, formation of amorphous high-energy states, and polymer-mediated supersaturation/precipitation inhibition [10]–[12]. Contemporary understanding emphasizes that release from SDs may proceed through dissolution into a polymer-rich boundary layer and/or liberation of drug-rich particles whose behavior depends on carrier dissolution kinetics and drug–polymer interactions [13], [14].

The routine use of SDs as an approach to improve the oral bioavailability of BCS class II drugs, the majority of which are absorption limited by dissolution, has been established through multiple protocols [10]–[12], [14], with common carriers being polyvinylpyrrolidone (PVP), polyethylene glycols (PEGs), and other hydrophilic or amphiphilic polymers selected for the properties of miscibility, glass transition behavior, resistance to recrystallization, and ease of manufacture [11], [14]. While SDs have many advantages, they can be difficult to develop because of the risks of phase separation, recrystallization, and the variability of the process; this variability may lead to changes in the dissolution profiles of the final product during either shelf life or scale-up [14]. These challenges necessitate predictive approaches to the dissolution behavior of SDs to provide early indicators of dissolution behavior.

Machine learning (ML) has evolved into a disruptive technology in pharmaceutical research allowing models to find predictive patterns in data rather than to rely on pre-specified mechanistic assumptions. As noted in several recent reviews, ML continues to expand its role across formulation development including accelerated screening, the optimization of formulation and process variables, and the integration of ML into automation and "self-driving" experimentation paradigms [15], [16]. Since dissolution profiles are inherently multivariate, and since dissolution profiles are the result of non-linear interactions among material characteristics (e.g., particle size distribution, polymer molecular weight, drug load, and crystallinity), process variables (e.g., compression force, mixing, and drying conditions), and testing conditions (e.g., pH of the dissolution medium and hydrodynamics), the attractiveness of ML to researchers studying dissolution science is clear.

Recent studies have shown the application of ML to predict: i) the entire drug-release profile based upon formulation composition and manufacturing variables and ii) kinetic parameters (e.g., Weibull) that can be reconstructed into release curves providing both predictive capability and interpretability [17]. Artificial neural networks (ANNs) have been successfully applied to predict dissolution profiles of solid oral dosage forms and have the potential to outperform linear baselines when non-linearities are dominant [18]. Additionally, data-driven approaches utilizing raw-material databases and modern feature attribution methods have been utilized to predict dissolution time or release-related endpoints supporting explainability and formulation insights [19], [20]. Furthermore, ML has been applied to predict dissolution performance in a broader manufacturing context (e.g., additive manufacturing/3D printing), demonstrating the ability of ML to generalize across disparate formulation datasets [21]. Compared to traditional modeling, ML provides: i) increased accuracy in systems where non-linearity dominates, ii) rapid in silico screening of candidate formulations, iii) the ability to identify critical drivers of dissolution behavior via model interpretation, and iv) potentially reduced experimental burdens while maintaining alignment with established dissolution metrics and regulatory requirements [4], [5], [17].

Glipizide, a second-generation sulfonylurea used to treat type-2 diabetes, presents a classic formulation challenge: it is practically insoluble in water, and its oral performance can be limited by dissolution and solubility constraints consistent with BCS class II behavior reported throughout the formulation literature [22]. Experimental studies further characterize its weak, solvent-dependent aqueous solubility [23], underscoring the need for solubility-enhancing strategies [24].

SDs of glipizide prepared using polymers such as PVP and PEG have been extensively studied to increase solubility and dissolution rate, with studies reporting enhanced release in relevant dissolution media and providing evidence of solid-state changes characterized by spectroscopic and thermal methods [22]. Similarly, earlier studies examined carrier-based dispersions (e.g., PEG, mannitol, and PVP) and demonstrated improvements in dissolution behavior relative to crystalline drug or physical mixtures [25]. Glipizide SDs can exhibit dissolution behavior that is formulation-dependent due to the effects of drug loading, polymer grade, and the degree of amorphization or drug-polymer interaction. Thus, these SDs represent an ideal example of a system for which ML-based predictive capabilities would be beneficial. Through learning from experimental datasets encompassing different polymer types, ratios, and processing routes, ML models can assist in identifying regions of formulation space that are likely to produce desired dissolution profiles, while minimizing iterative trial-and-error experimentation [25]–[28].

Despite this progress, prior ML studies of dissolution have largely targeted single-point or endpoint outcomes, have focused on tablet or 3D-printed systems, or have relied on large heterogeneous datasets mined across many drugs. Where SD dissolution profiles have been modeled, it has typically been within large-scale screening platforms in which generalization to individual unseen formulations is not evaluated under leakage-controlled validation. It therefore remains unclear how faithfully standard ML and sequence models can reconstruct the full dissolution trajectory of SD formulations of a single poorly soluble drug when tested under strict formulation-level holdout—the regime most relevant to early screening. This study addresses that gap for glipizide SDs.

The three contributions of this study are: to the academic world, to practitioners, and to the researcher. First, rather than considering only the dissolution endpoint, it treats SD dissolution prediction as a ‘full dissolution-profile regression problem’. Analysis is based on a standard dataset of 16 glipizide SD formulations, made using three different polymer types and four different ratios of drug-to-polymer, allowing the models to learn relationships between formulation and time for the entire release profile. Second, the study compares under the same evaluation framework five different modelling approaches: bagged trees, least squares boosting (LSBoost), support vector regression (SVR), Gaussian process regression (GPR), and a long short-term memory (LSTM) sequence-to-sequence network. Grouped cross-validation was carried out at the formulation level to minimize time-point leakage and to ensure the different time points for each formulation were not split between the training and testing sets, giving a more realizable estimation of formulation level generalization. Third, the study assesses the transferability and reproducibility of the proposed modeling framework, which provides a template that may be relevant for modeling other SD systems, and not just a specific prediction for a given drug.

This study makes several significant contributions to the previous ML studies on dissolution prediction. Large-scale studies have shown that the dissolution profile of SD can be predicted by ML algorithms, such as random-forest regression, based on hundreds of dissolution profiles measured in different drugs. The present work, on the other hand, uses a ‘controlled single-drug benchmark’ that enables the behavior of various model families to be analyzed under a single holdout strategy for the formulation level and under a well-defined formulation space. This design aims at methodological transparency and reproducibility and minimizes potential confounding by drug, data and experimental source differences. Moreover, this study is specifically designed to address the complete dissolution trajectory, instead of endpoint properties, like dissolution time or maximum release, losing information on the release rate, curve shape and temporal behavior. Conventional tabular and kernel-based approaches and a sequence-to-sequence LSTM model are also included as another distinguishing feature. Most previous comparative research has focused mostly on tree-based or traditional regression algorithms and relatively few studies have assessed sequence-learning algorithms with the same validation procedure. This study aims to compare ensemble, kernel-based, probabilistic and sequence-learning approaches to dissolution-profile prediction through the evaluation of four related algorithms in a common framework: bagged trees, LSBoost, SVR, and LSTM. Together these design features offer a reusable platform to evaluate ML models when evaluated in the formulation level generalization setting and serve as a starting point for further studies that employ larger, multi-drug, experimentally generated dissolution datasets.

2. MATERIALS AND METHODS

2.1. Dataset

The modeling data were derived from the published glipizide SD study of Alotaibi *et al.* [22]. Two distinct categories of information were extracted. First, the percent drug-release versus time profiles—the primary modeling target—were obtained by point-by-point digitization of the dissolution curves reported in the figures of the study by Alotaibi *et al.* [22] using a graph-digitization tool (WebPlotDigitizer), sampled at t={0, 5, 10, 15, 30, 45, 60} min and constrained to 0–100%. Second, the per-formulation kinetic-fit descriptors (R^2 for zero-order, first-order, Higuchi, and Korsmeyer–Peppas models, and the Peppas exponent n) were taken as reported in the kinetic-analysis tables of the study by Alotaibi *et al.* [22] and used only as auxiliary features; they were never used to generate or reconstruct the release values. Keeping the release-time series (target) and the kinetic descriptors (predictors) as independent representations avoids any circularity. Coincident digitized points at a formulation–timepoint were averaged, and negative values arising from digitization noise were set to zero.

2.1.1. Formulation set and identifiers

Sixteen formulations were modeled: twelve SDs prepared with three polymers at four drug:polymer ratios (F1–F4 for PVP K30, FP1–FP4 for PVP K90, G1–G4 for PEG 6000), plus reference/tablet curves (GP and GP_SD) and optimized-tablet curves (TF4 and TFP4). Formulation metadata were derived deterministically from the identifier (PolymerType, Ratio, and DosageForm). Table 1 depicts the formulation metadata mapping used for ML feature construction.

Table 1. Formulation metadata mapping used for ML feature construction

FormulationID	PolymerType	Ratio (1:x)	DosageForm
F1	PVP_K30	1	SD
F2	PVP_K30	2	SD
F3	PVP_K30	3	SD
F4	PVP_K30	4	SD
FP1	PVP_K90	1	SD
FP2	PVP_K90	2	SD
FP3	PVP_K90	3	SD
FP4	PVP_K90	4	SD
G1	PEG_6000	1	SD
G2	PEG_6000	2	SD
G3	PEG_6000	3	SD
G4	PEG_6000	4	SD
GP	NONE	0	TABLET
GP_SD	NONE	0	SD/reference
TF4	PVP_K30	4	TABLET
TFP4	PVP_K90	4	TABLET

2.1.2. Dissolution time-series dataset (DissolutionLong)

The primary label dataset is a long-format dissolution table in which each row corresponds to one formulation at one timepoint. As described in subsection 2.1, percent-release values were digitized from the dissolution figures of the study by Alotaibi *et al.* [22] at t={0, 5, 10, 15, 30, 45, 60} min (t=0 included as a baseline where used). The target variable is ReleasePct (percent drug released). The DissolutionLong schema is shown in Table 2.

Table 2. DissolutionLong schema

Column	Type	Description
FormulationID	string/categorical	Unique formulation identifier (e.g., F1, FP4, G3, TF4, GP, GP_SD)
TimeMin	numeric	Sampling time in minutes (e.g., 0, 5, 10, 15, 30, 45, 60)
ReleasePct	numeric	Percent drug released at TimeMin (0–100)

2.1.3. Kinetic descriptor dataset

A second dataset contains per-formulation kinetic fitting descriptors reported in study by Alotaibi *et al.* [22]: R^2 values for zero-order, First-order, Higuchi, and Korsmeyer–Peppas models, and the Peppas exponent n. A categorical BestFitModel feature is derived per formulation as the model with the maximum R^2. Tablet descriptors are available for TF4, TFP4, and GP as demonstrated in Table 3 which shows the schema (per-formulation descriptors).

Table 3. Schema (per-formulation descriptors)

Column	Type	Description
FormulationID	string/categorical	Join key to dissolution dataset
R2_ZeroOrder	numeric	R^2 for zero-order fit
R2_FirstOrder	numeric	R^2 for first-order fit
R2_Higuchi	numeric	R^2 for Higuchi model
R2_KorsmeyerPeppas	numeric	R^2 for Korsmeyer–Peppas model
n_Peppas	numeric	Peppas release exponent (n)
BestFitModel	categorical (derived)	Argmax of the four R^2 values (Zero/First/Higuchi/Peppas)

2.1.4. Derived machine learning-ready dataset (merged+engineered features)

The ML-ready dataset is obtained by merging DissolutionLong with Table 3 using FormulationID, then adding deterministic formulation metadata and engineered time features. The resulting table contains one row per formulation-timepoint with both predictors and the ReleasePct label as seen in Table 4 which depicts the feature groups used in the ML-ready table.

Table 4. Feature groups used in the ML-ready table

Feature group	Variables
Formulation metadata	Polymer type (categorical), Ratio (numeric), Dosage form (categorical)
Time features	TimeMin (numeric), log(TimeMin), sqrt(TimeMin)
Interaction feature	Polymer type ratio (categorical)
Kinetic descriptors (optional)	R2_ZeroOrder, R2_FirstOrder, R2_Higuchi, R2_KorsmeyerPeppas, n_Peppas, BestFitModel
Target label	ReleasePct

2.1.5. Data lineage and processing diagram

The workflow diagram summarizes how the curated dissolution dataset was constructed and analyzed for dissolution prediction. It shows the transformation from reference-study information into standardized tables, followed by identifier normalization, feature engineering, grouped cross-validation by formulation, and model training/evaluation. The dataset lineage and ML analysis workflow are shown in Figure 1.

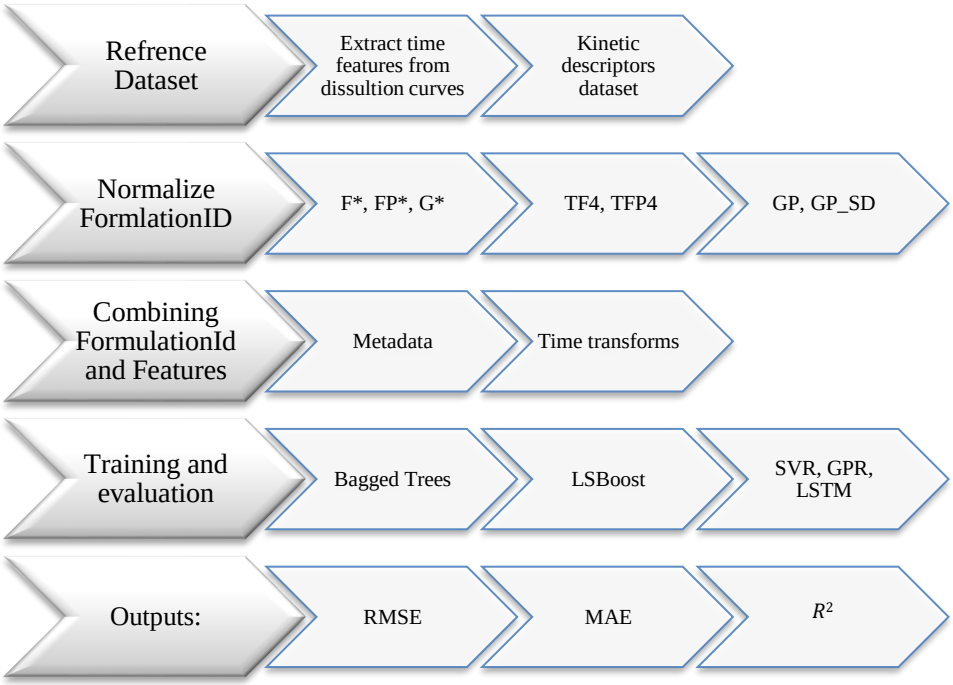


Figure 1. Dataset lineage and ML analysis workflow

2.2. Preprocessing and missing-data handling

To ensure robust training on a small dataset, missing numeric predictors were imputed using the median value computed on the training fold only (to avoid test leakage). Missing categorical predictors were assigned an explicit 'Unknown' category. For models sensitive to feature scaling (GPR, SVR, and LSTM), predictors were z-score standardized using the training-fold mean and standard deviation, and the same parameters were applied to the corresponding test fold.

2.3. Machine learning and deep learning models

The target variable was ReleasePct, modeled as a function of formulation predictors and time. The following models were trained and compared: i) bagged trees (random forest-style ensemble of regression trees), ii) LSBoost (gradient boosting with regression trees), iii) SVR with a Gaussian kernel, iv) GPR with an automatic relevance determination (ARD) squared-exponential kernel, and v) an LSTM-based sequence-to-sequence regression model to predict full dissolution trajectories.

2.4. Grouped cross-validation and leakage control

To prevent information leakage across timepoints from the same formulation, model evaluation used grouped K-fold cross-validation with grouping by FormulationID, ensuring that all timepoints for a given formulation were assigned to the same fold. This design evaluates generalization to unseen formulations rather than unseen timepoints of known formulations. Because each formulation contributes multiple observations—one per sampling time—random record-level partitioning would place timepoints from the same formulation in both training and test folds, allowing a model to reconstruct held-out timepoints by interpolating among its own training points and producing optimistic error estimates. Grouping by FormulationID ensures all timepoints of a formulation share one fold and each formulation appears in the held-out set exactly once, so the estimate reflects generalization to unseen formulations. All data-dependent preprocessing (median imputation, z-score standardization) was fitted on training folds only.

2.5. Performance metrics and visual diagnostics

Predictive performance was quantified using root mean square error (RMSE), mean absolute error (MAE), and coefficient of determination (R^2) computed on held-out folds. In addition to overall metrics, per-formulation metrics were computed to identify formulation-specific generalization failures. Diagnostic plots included predicted-versus-true scatter plots, residuals versus time (pred-true), and grouped dissolution curve overlays organized by formulation family (F, FP, G, and reference/tablet set). Figure 2 demonstrates the analysis method structure of the prepared dataset.

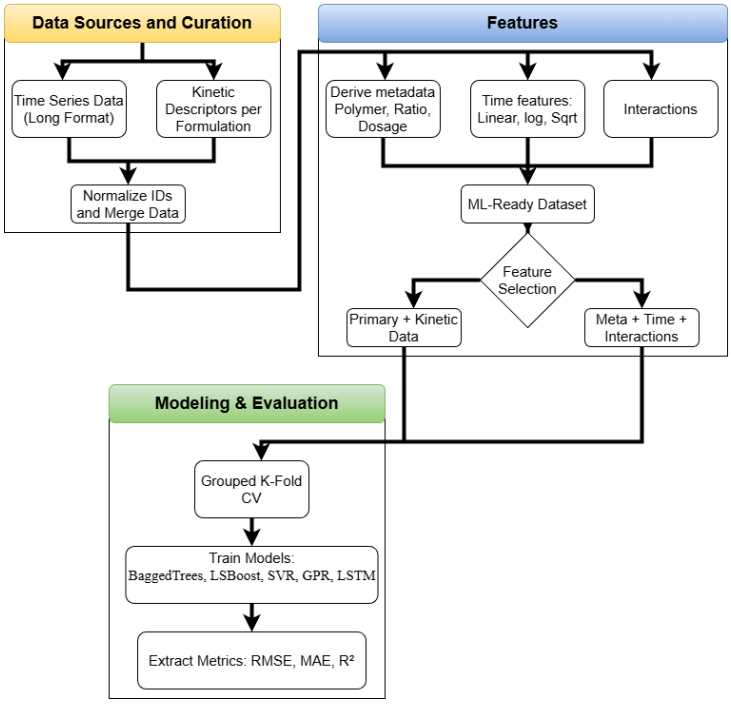


Figure 2. Analysis structure of the prepared dataset

2.6. Implementation, hyperparameters, and reproducibility

All modeling was performed in MATLAB R2024a using the statistics and ML toolbox and the deep learning toolbox, with a fixed Mersenne Twister seed (rng(42)) governing fold assignment and all stochastic operations; predicted release was clipped to 0–100%. The reported models used thirteen predictors: three-time features (TimeMin, log(TimeMin), sqrt(TimeMin)), the numeric drug:polymer ratio, three categorical descriptors (PolymerType, DosageForm, and their interaction), and six kinetic descriptors, with categorical one-hot encoded against a fixed category list including an explicit "Unknown" level. Within each fold, missing numeric predictors were median-imputed and missing categorical set to "Unknown" using training-partition statistics only; for scale-sensitive models (GPR, SVR, and LSTM) predictors were z-score standardized on training folds and applied to the held-out fold, while tree ensembles used unscaled predictors. Grouped 5-fold cross-validation assigned the 16 formulations round-robin to folds of 4/3/3/3/3, and metrics were pooled over out-of-fold predictions. Hyperparameters were fixed a priori for this small dataset; kernel models used MATLAB's heuristic ("auto") kernel scale and default regularization. Model settings are summarized in Table 5.

Table 5. Model configurations and hyperparameters

Model	Configuration
Bagged trees	fitrensemble, Bag; 200 cycles; regression-tree learners, min leaf size 3; all predictors per split; unscaled inputs
LSBoost	fitrensemble, LSBoost; 400 cycles; learn rate 0.05; regression-tree learners, min leaf size 3; unscaled inputs
SVR	fitrsvm, Gaussian kernel; kernel scale=auto; box constraint and ε at defaults; z-scored inputs
GPR	fitrgp, ARD squared-exponential kernel; constant basis; length scales by marginal-likelihood maximization; z-scored inputs
LSTM	sequenceInputLayer→lstmLayer(32, sequence)→fullyConnectedLayer(1)→regression; Adam; 400 epochs; mini-batch 4; initial LR 5×10^{-3}; gradient threshold 1; shuffle every epoch; CPU

3. RESULTS

Model performance was evaluated using grouped 5-fold cross-validation at the formulation level (16 unique formulations; all timepoints from a formulation were kept within the same fold). Figures 3 and 4 provide complementary scatter and residual diagnostics.while Figures 5–9 summarize out-of-fold reconstruction of dissolution curves by formulation family for the bagged trees, LSTM, LSBoost, SVR, and GPR models.

3.1. Overall predictive performance (predicted vs. true release)

Predicted-versus-true release is shown in Figure 3 for out-of-fold predictions under grouped cross-validation, with panels (a)–(e) corresponding to bagged trees, LSTM, LSBoost, SVR, and GPR, respectively. The panels reveal clear differences in model calibration and in the ability to span the full release range (0–100%). Bagged trees achieved the best overall performance (RMSE=18.90%; MAE=14.03%; R^2=0.701; Figure 3(a)), closely followed by the LSTM (RMSE=19.18%; MAE=12.42%; R^2=0.692; Figure 3(b)). LSBoost performed moderately (RMSE=21.23%; MAE=14.13%; R^2=0.623; Figure 3(c)), with larger dispersion at intermediate release levels. In contrast, SVR and GPR exhibited marked underfitting: Figures 3(d) and (e) show that both models produced near-constant predictions across a wide span of true release values, yielding negative coefficients of determination (SVR R^2=−0.081; GPR R^2=−0.377). This is consistent with collapse toward an average prediction and failure to capture nonlinear formulation–time interactions. In summary, tree ensembles and the LSTM spanned the full release range, whereas SVR and GPR collapsed toward near-constant predictions.

3.2. Cross-validated performance metrics

Table 6 outlines the pooled out-of-fold predictive performance metrics for all evaluated models, aggregated across cross-validation folds to provide a robust estimate of generalization performance, with formulation-level bootstrap 95% confidence intervals. Models are ranked in ascending order of RMSE, lower being better. In summary, bagged trees and the LSTM achieved the lowest errors with overlapping confidence intervals, while SVR and GPR gave negative R^2.

3.3. Time-dependent error structure (residuals vs. time)

Figure 4 shows the residuals (predicted−true, % release) versus time for out-of-fold predictions under grouped cross-validation, used to assess time-dependent bias and dispersion: bagged trees in Figure 4(a), LSTM in Figure 4(b), LSBoost in Figure 4(c), SVR in Figure 4(d), and GPR in Figure 4(e).

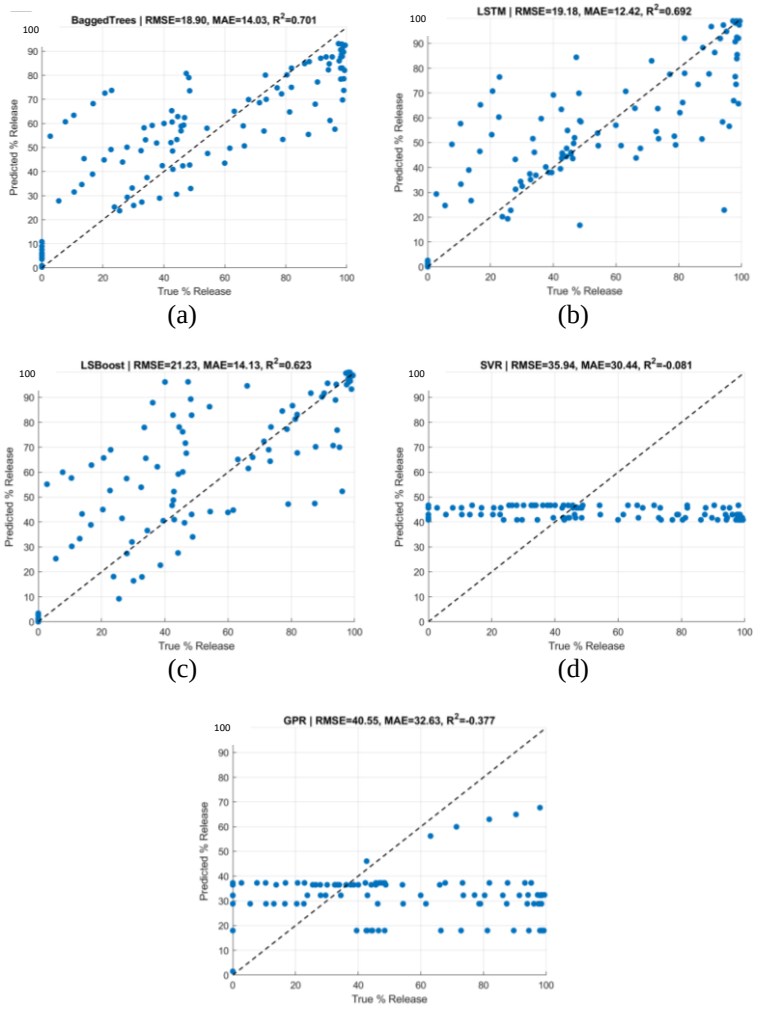


Figure 3. Predicted versus true dissolution (% release) for out-of-fold predictions under grouped cross-validation; (a) bagged trees, (b) LSTM, (c) LSBoost, (d) SVR, and (e) GPR

Table 6. Reports pooled out-of-fold performance metrics for each model ordered by RMSE

Model	RMSE (% release)	95% CI (RMSE)	MAE (% release)	R^2
Bagged trees	18.90	[12.6, 25.9]	14.03	0.701
LSTM	19.18	[13.2, 24.9]	12.42	0.692
LSBoost	21.23	[14.2, 27.5]	14.13	0.623
SVR	35.94	[29.9, 41.6]	30.44	-0.081
GPR	40.55	[30.1, 49.9]	32.63	-0.377

Bagged trees and LSTM were generally centered near zero across sampling times, indicating limited systematic bias as a function of time. However, both models exhibited occasional large outliers, consistent with formulation-specific generalization errors when an entire formulation curve is held out during grouped cross-validation. Additionally, LSBoost showed a similar overall pattern but with more frequent positive residuals at later timepoints (30–60 min), suggesting a tendency to overestimate late-time approach to plateau for certain formulations. SVR and GPR showed strong systematic structure: positive residuals for low-release observations and negative residuals for high-release observations, consistent with near-constant predictions and under fitting. Taken together, the scatter and residual diagnostics indicate that tree ensembles and the LSTM sequence model best captured the nonlinear dissolution dynamics in this dataset under strict formulation-level evaluation. In summary, the leading models were largely unbiased over time apart from occasional formulation-level outliers, while SVR and GPR showed the low-then-high residual signature of mean reversion. Table 6 reports pooled out-of-fold performance metrics.

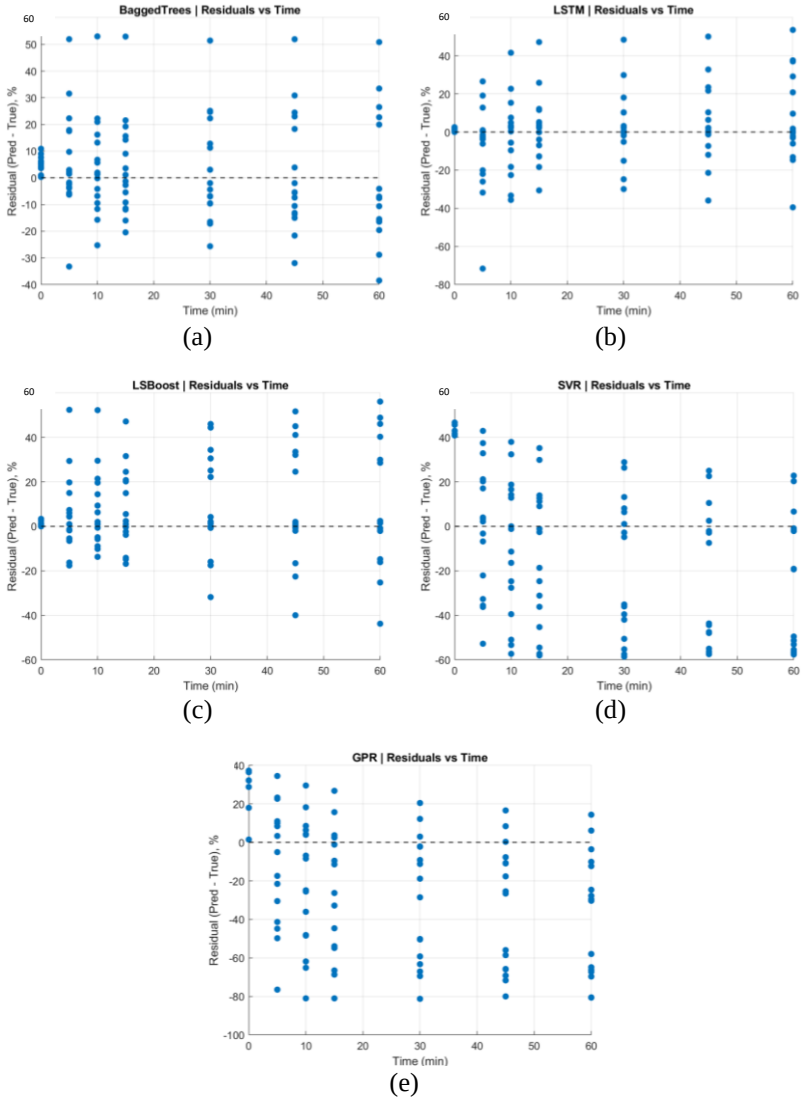


Figure 4. Residuals (predicted−true, % release) versus time for out-of-fold predictions under grouped cross-validation; (a) bagged trees, (b) LSTM, (c) LSBoost, (d) SVR, and (e) GPR

3.4. Grouped dissolution curve reconstruction by formulation family

To evaluate whether models reproduced complete dissolution curve shapes across polymer families, observed and predicted profiles were overlaid within four formulation groups, Figures 5–9. The solid line represents a profile observed (digitized) while the dashed line represents an out-of-fold prediction; markers differentiate formulations; panels (a)–(d) refer to PVP K30 (F1–F4), PVP K90 (FP1–FP4), PEG 6000 (G1–G4), and reference/tablet profiles (GP, GP_SD, TF4, TFP4), respectively. Bagged trees, Figures 5(a)–(d), showed the least deviation from the PVP based dispersions (panels a, b, d) in terms of curve tracking, with a similar high early release rate and plateau observed for these groups, and with the slower, more gradual profiles observed for the PEG based dispersions (panel c). The largest deviations occurred in the reference/tablet panel (d) with GP and GP_SD being over-predicted at early/mid time points.

The LSTM sequence model Figures 6(a)–(d) reconstructed monotonic trends, and overall curvature, across groups, but occasionally smoothed steep early-time rises in fast formulations (e.g., F4/TF4), or misestimated the approach to plateau for specific withheld formulations, especially in the reference/tablet panel. LSBoost Figures 7(a)–(d) had similar qualitative trends, with overestimation of late-time release (30–60 min) more common within groups. By contrast, the predicted trajectories for the SVR and GPR were underfitted in the grouped curve overlays, Figures 8(a) to (d) and 9, resulting in a relatively small difference between polymer families.

Finally, Figure 9 showed the grouped dissolution curve reconstruction for the GPR model under grouped cross-validation by formulation. Figure 9(a) PVP K30 SDs (F1–F4), Figure 9(b) PVP K90 SDs (FP1–FP4), Figure 9(c) PEG 6000 SDs (G1–G4), and Figure 9(d) reference/tablet profiles (GP, GP_SD, TF4,

TFP4). Solid lines indicate observed (digitized) dissolution profiles and dashed lines indicate out-of-fold predictions; markers distinguish formulations within each panel. In summary, bagged trees most faithfully reproduced curve shape and preserved polymer-family separation.

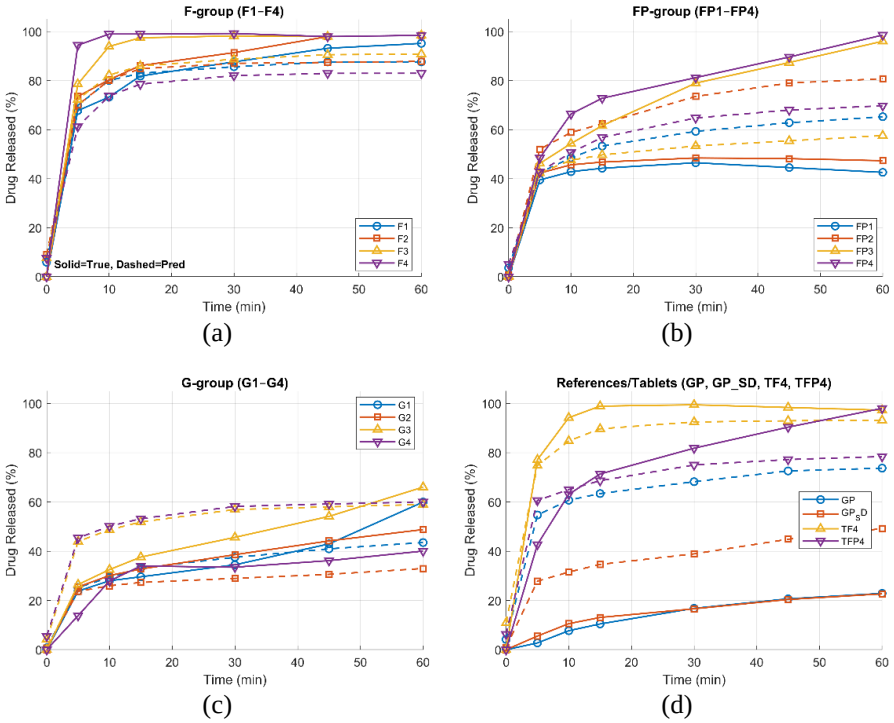


Figure 5. Grouped dissolution curve reconstruction-bagged trees; (a) PVP K30 (F1–F4), (b) PVP K90 (FP1–FP4), (c) PEG 6000 (G1–G4), and (d) (GP, GP_SD, TF4, TFP4)

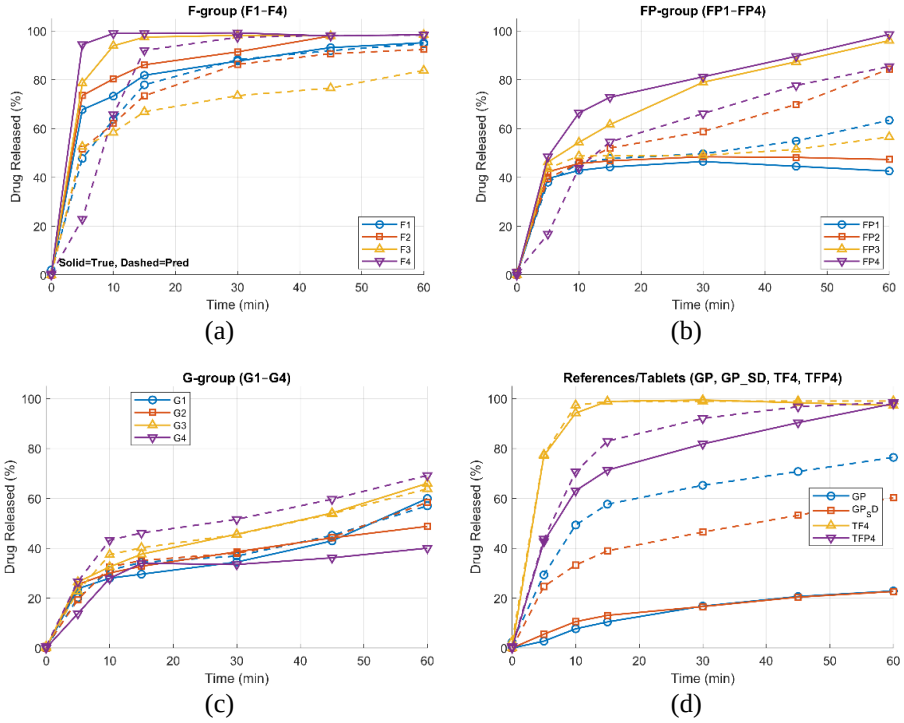


Figure 6. Grouped dissolution curve reconstruction—LSTM; (a) PVP K30 (F1–F4), (b) PVP K90 (FP1–FP4), (c) PEG 6000 (G1–G4), and (d) (GP, GP_SD, TF4, TFP4)

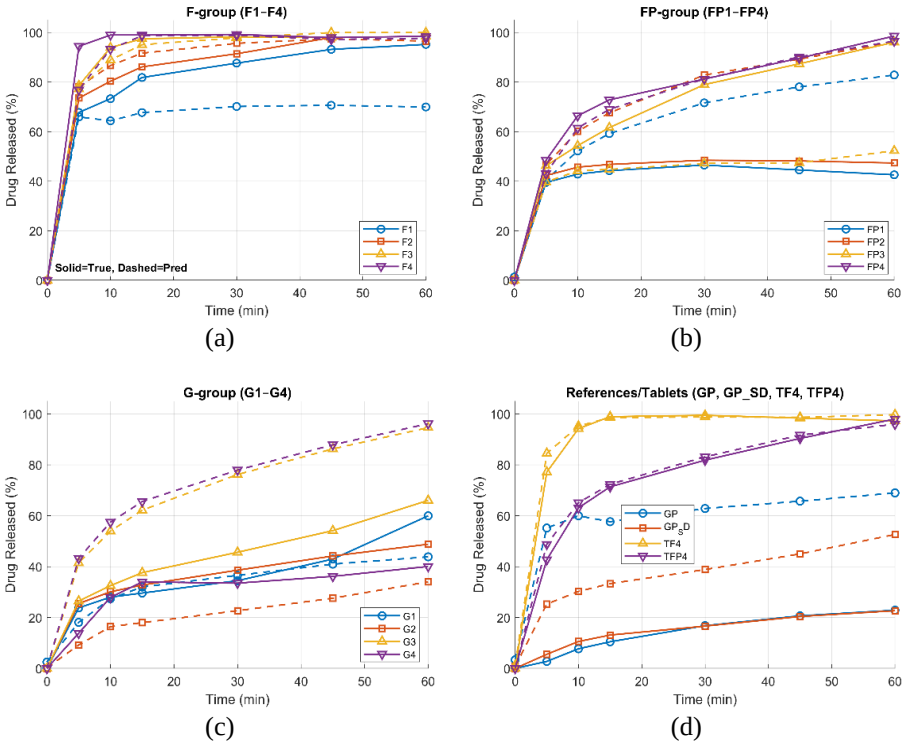


Figure 7. Grouped dissolution curve reconstruction—LSBoost; (a) PVP K30 (F1–F4), (b) PVP K90 (FP1–FP4),(c) PEG 6000 (G1–G4), and (d) (GP, GP_SD, TF4, TFP4)

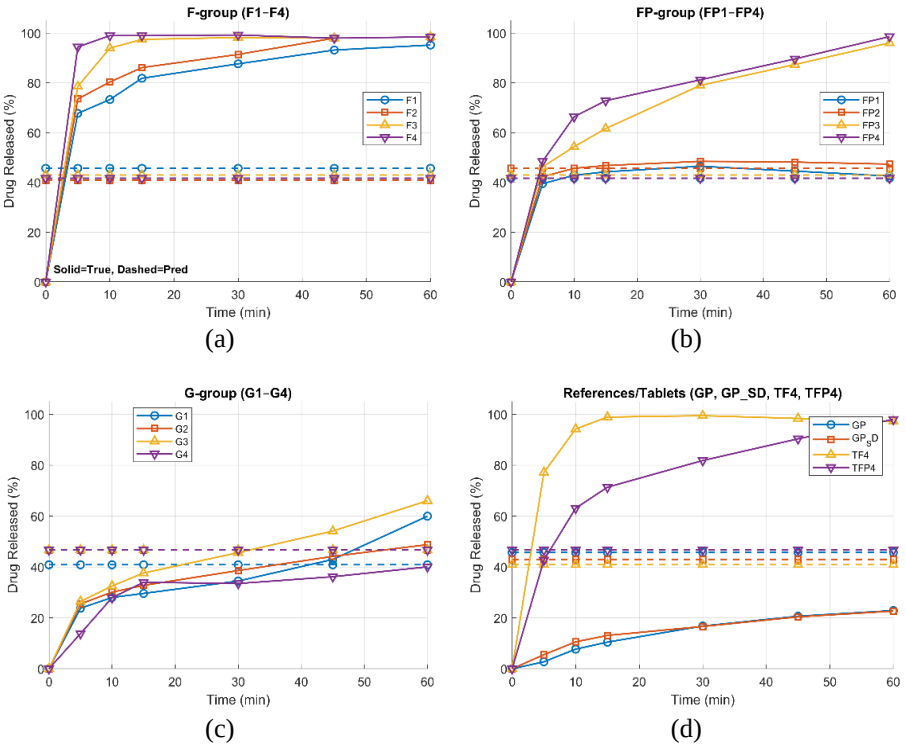


Figure 8. Grouped dissolution curve reconstruction—SVR; (a) PVP K30 (F1–F4), (b) PVP K90 (FP1–FP4), (c) PEG 6000 (G1–G4), and (d) (GP, GP_SD, TF4, TFP4)

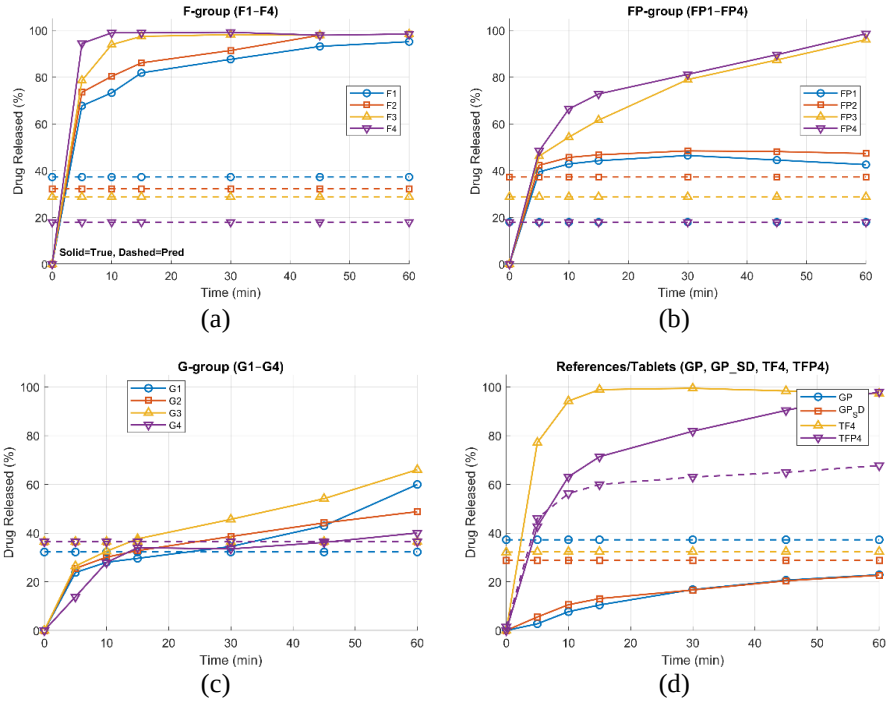


Figure 9. Grouped dissolution curve reconstruction; (a) PVP K30 (F1–F4), (b) PVP K90 (FP1–FP4), (c) PEG 6000 (G1–G4), and (d) (GP, GP_SD, TF4, TFP4)

3.5. Predictor importance

Permutation-based predictor importance for the bagged trees model is shown in Figure 10. Figure 10(a) shows top individualpredictors and Figure 10(b) shows importance aggregated by feature group. Aggregated by group, the time features (TimeMin, log, sqrt) accounted for the largest share (≈44%), followed by polymer type (≈36%), with ratio and the polymer×ratio interaction contributing ≈15% combined. The kinetic-fit descriptors together contributed less than 4% (the Peppas exponent n was effectively unused), indicating that predictions rest almost entirely on formulation and time descriptors. In summary, time and polymer identity dominated predictions, while kinetic descriptors contributed negligibly.

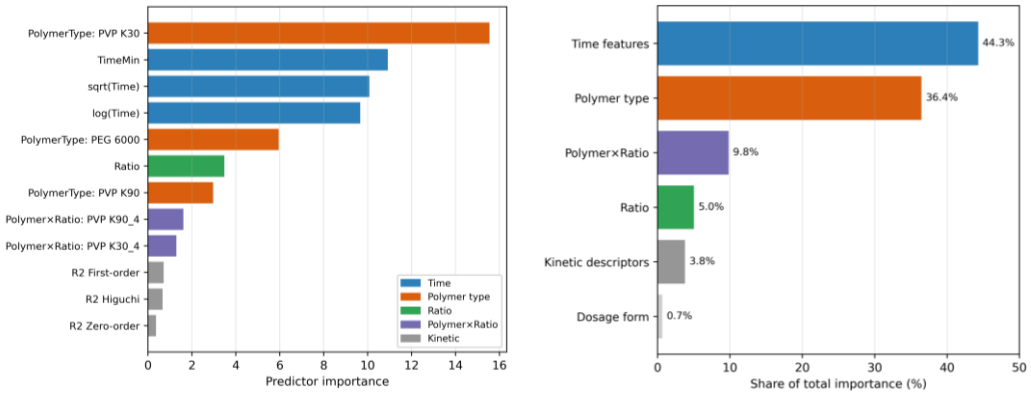


Figure 10. Permutation predictor importance for the bagged trees model; (a) top individual predictors and (b) importance aggregated by feature group

3.6. Feature ablation (kinetic descriptors)

To confirm the leading models do not depend on the kinetic descriptors (which share a source with the digitized curves), the full grouped cross-validation was repeated using only formulation and time features.

The primary configuration (with kinetic descriptors) corresponds to Table 5; formulation-only results are reported in Table 7. Consistent with the feature-importance analysis (subsection 3.5), the accuracy and ranking of the leading models are preserved when the kinetic descriptors are removed.

Table 7. Feature ablation: primary (with kinetic descriptors) versus formulation-only configuration

Model	RMSE (primary)	R^2 (primary)	RMSE (formulation-only)	R^2 (formulation-only)
Bagged trees	18.90	0.701	12.1468	0.7651
LSTM	19.18	0.692	11.6152	0.7556
LSBoost	21.23	0.623	14.0935	0.6213
SVR	35.94	-0.081	22.6720	0.1515
GPR	40.55	-0.377	30.40	-0.0842

4. DISCUSSION

This study developed ML models to predict complete in vitro dissolution profiles (percent release over time) for glipizide SDs using formulation descriptors (polymer type, drug:polymer ratio, and dosage-form class), engineered time variables, and, when available, kinetic-fit descriptors. This objective reflects the continuing importance of dissolution profiling for guiding formulation development, while acknowledging that conventional curve-comparison metrics and kinetic fitting can be inadequate when dissolution is governed by high-dimensional, non-linear interactions among material and formulation attributes [6], [7]. SDs exemplify this challenge because polymer selection, drug–polymer interactions, and physical stability processes (e.g., amorphization, phase separation, recrystallization) can markedly alter dissolution in ways that are difficult to anticipate using simple mechanistic or empirical models [12], [14]. Accordingly, accurate predictive models can support more efficient formulation screening and rational selection of carriers and ratios for poorly soluble drugs such as glipizide [18]. Methodologically, dissolution prediction was treated as a profile-level learning task rather than a single-point endpoint. ReleasePct was modeled across multiple timepoints using a long-format dataset (one formulation–timepoint per observation) and targeted feature engineering, including logarithmic and square-root time transforms, polymer–ratio interaction terms, and optional kinetic descriptors. Multiple model classes were evaluated to capture potential nonlinearities and saturation effects typical of dissolution data, including tree ensembles (bagged trees, LSBoost), kernel methods (SVR with Gaussian kernel; GPR with ARD squared-exponential kernel), and an LSTM sequence-to-sequence architecture. Performance was assessed using grouped K-fold cross-validation by FormulationID to prevent time point leakage and to quantify generalization to unseen formulations, which is the relevant use case for formulation screening.

4.1. Factors influencing model performance

The performance ordering follows from each model's inductive bias and the size and structure of the dataset. Tree ensembles represent the release surface as piecewise-constant partitions of the joint formulation–time space, capturing threshold-like and interaction effects without feature scaling or an assumed functional form; bagging reduces variance, advantageous for a small, digitization-noisy dataset. Bagged trees marginally exceeded LSBoost, consistent with gradient boosting's tendency to overfit residuals on scarce data—visible as LSBoost's positive late-time bias. The LSTM performed comparably because a sequence-to-sequence formulation encodes temporal order and the characteristic rise-and-plateau of dissolution curves; with only 16 short sequences it tended to smooth steep early-time rises. The underfitting of SVR and GPR is attributable to default/heuristic hyperparameters on a small, one-hot-expanded feature space rather than intrinsic unsuitability of kernel methods: SVR over-regularizes and collapses toward the mean, while the ARD-GPR drives its length scales large and reverts to the constant basis. Both show the low-then-high residual signature of regression to the mean, and both would be expected to improve with dedicated hyperparameter optimization. Table 8 depicts summary of model strengths and characteristic failure modes.

Table 8. Summary of model strengths and characteristic failure modes

Model	Strengths	Weakness/failure mode
Bagged trees	Best accuracy; captures nonlinear interactions; no scaling or tuning needed	Occasional formulation-level outliers; limited extrapolation
LSTM	Comparable accuracy, lowest MAE; encodes temporal shape	Data-hungry; smooths early rises; least interpretable
LSBoost	Moderate accuracy; captures interactions	Overfits residuals on small data; positive late-time bias
SVR	Effective in principle for nonlinear regression	Over-regularized under defaults; mean-reverting
GPR	Provides predictive uncertainty intervals	Severe underfitting; ARD collapses on scarce data; most negative R^2

4.2. Formulation and polymer-family trends

The general predicted pattern of release was mechanistically reasonable based upon the formulation variables. This study evaluated dispersions made from three different polymers (PVP K30, PVP K90, and PEG 6000) using multiple drugs to polymer ratios as well as reference/tablet profiles. The stronger predictive models demonstrated wide-ranging differences based upon polymer, and PVP-based formulations typically exhibited faster release and earlier onset of a plateau compared to the more gradual dissolution profiles observed with PEG-based formulations. The latter observation is consistent with previous evidence demonstrating that chemical and physical properties of polymers (molecular weight, chemical composition), as well as their effects on amorphization, wettability, matrix dissolution, and precipitation inhibition, can significantly impact the performance of SDs [14]. Furthermore, inclusion of kinetic fit descriptors in the model provided additional evidence of how traditional methods of interpreting dissolution data could be applied to predicting dissolution data using data driven approaches, as has been recently reported in studies of pharmaceuticals [19].

4.3. Statistical comparison and model selection

To quantify uncertainty given the small number of formulations, formulation-level (cluster) bootstrap 95% confidence intervals were computed for each model's RMSE (2,000 resamples; Table 5). The intervals are wide: bagged trees [12.6, 25.9], LSTM [13.2, 24.9], and LSBoost [14.2, 27.5] overlap substantially, whereas SVR [29.9, 41.6] and GPR [30.1, 49.9] are clearly separated. A paired bootstrap of the two leading models found their RMSE difference indistinguishable from zero (95% CI [−3.67, 2.57]; P(difference≥0)=0.44). We therefore do not claim a single best model: bagged trees and the LSTM are statistically indistinguishable, and both clearly outperform the kernel methods.

4.4. Outlier and failure-mode analysis

Errors were concentrated in a few formulations. For both leading models the largest error occurred for the pure-drug reference GP (bagged trees RMSE 48.2; LSTM 42.1), with GP_SD and the most extreme drug: polymer ratios (G4, FP3, F4) also among the worst-predicted. These are singletons in feature space—the only pure-drug references and edge-of-range ratios—so under grouped holdout the model must predict a descriptor combination unrepresented in the training folds. The resulting large level errors are an expected consequence of leave-one-formulation-out evaluation on a small, unbalanced set and should diminish as additional formulations are added.

4.5. Comparison with prior machine learning dissolution studies

Accuracy should be read in the context of the evaluation regime. Large-scale platform studies have reported higher accuracy using random forests [26], but on datasets one to two orders of magnitude larger and without single-formulation holdout; both inflate apparent performance relative to the present16-formulation, leakage-controlled setting. Studies predicting endpoint quantities such as dissolution time [20], or the profiles of tablet and extended-release systems [18], [19], address different targets. An $R^2 \approx 0.70$ for full-curve prediction of unseen glipizide dispersions under strict grouped cross-validation is thus a conservative but honest estimate.

4.6. Practical implications for formulation screening

Such models could be validated at scale with larger, more diverse, and independently produced datasets and then become an in-silico screening tool at an early stage for the development of glipizide SD. The models could predict complete dissolution profiles for various types of carriers and drug-to-polymer ratios, help prioritize formulations for further laboratory testing, and rank the formulations by their expected dissolution performance. Having this capability could significantly decrease the number of formulations that must be prepared physically and tested in the initial screening phase, thus eliminating the need for experimental time, materials, and resources. The predicted dissolution trajectories may also serve as a more informative justification for choosing the formulation(s) for a new drug product than an endpoint analysis alone, as the researchers can compare the differences in release rates, dissolution shapes, and overall release behavior between the candidate formulations. In addition, they might be used to optimize formulation factors using design-of-experiments (DoE) methodology and explore areas of the formulation space that have the greatest potential for success. For instance, the model predictions could be used to prioritize combinations of prediction which may be best suited to obtain a desired dissolution profile before deciding to proceed with experimental preparation.

Importantly, the approach proposed should be considered as a decision support and prioritization tool and not as a substitute for experimental dissolution testing. Laboratory testing is still needed to verify predicted profile, unexpected formulation behavior, and to verify reproducibility. ML predictions could thus

offer a mid-stage screening stage between formulation design and experimental validation, in the context of a practical development flow. Proper external and prospective validation, the integration could support to better and more data-driven formulation optimization and facilitate the early development of poorly water-soluble drug delivery systems.

4.7. Transferability

The protocol is drug-agnostic in construction, relying on formulation descriptors, engineered time features, and optional general formulation descriptors, engineered time-related features, and optional kinetic descriptors are used for the proposed modeling protocol and are not variables that are specifically drug related to glipizide. The computational paradigm can therefore be easily transferred to other drugs with low water solubility, especially those with dissolution-limited bioavailability that are classified in the BCS class II. The current formulation and dissolution data could be replaced with data from another drug, so that the preprocessing, feature construction, model training, and validation at the formulation level procedures could be reused with relatively minor modifications. Transferability can also be extended to a wider scope of carrier materials, polymer families, drug-to-carrier ratios, and formulation conditions. But the transfer of the pipeline should not be taken for granted due to its drug agnostic structure. The relationships learned by these models may significantly change due to variations in drug physicochemical properties, polymer–drug interactions, crystallinity, particle properties, manufacturing processes, and dissolution mechanisms. Accordingly, any changes to the framework, such as retraining or fine-tuning, would likely be required if the framework were to be applied to a new drug, or to a substantially different formulation space. The limited number of formulations in the present dataset (16) is also significantly limiting to transferability. The more and varied the independent formulations, the more the models would have a wide variety of formulation–dissolution relationships to draw on and the better chance of being able to generalize to a new set of formulations they have not seen before. More experimental raw data, repeat dissolution experiments, more time points and a wider range of formulation conditions could further enhance model robustness. Kinetic descriptors, none specific to glipizide. In principle the same pipeline could apply to other BCS class II drugs and additional carriers, with performance expected to improve as the number of formulations grows beyond the present 16. Transfer to markedly different release mechanisms would require retraining, and external validation on an independent dataset remains the key next step.

4.8. Limitations

There are some limitations in this study. First, only 16 formulations were sampled, further reducing the power of the statistical models and the generalizability of the models because of the formulation level cross-validation. Second, the dissolution profiles were digitized from published values, and this could lead to errors in comparison to raw experimental measurements. Third, the data was limited to a few polymers and polymer-to-drug ratios, limiting the applicability of the data to other formulation situations. Additionally, dissolution was only measured at seven time points, which does not allow for detailed release behavior. Lastly, this study was retrospective in nature and did not have prospective experimental or external validation. As a result, larger and more diverse datasets, raw experimental measurements, and prospective validation are needed to ensure the reliability of the use of the models for pharmaceutical formulation optimization.

4.9. Future work

The most immediate priority is to enlarge and diversify the dataset—spanning additional drugs, carriers, and processing routes—which would narrow the confidence intervals and enable systematic hyperparameter optimization. External validation against independently measured dissolution profiles, and ultimately prospective testing on newly prepared formulations, is required before deployment. Coupling the data-driven models with mechanistic or kinetic descriptors in a hybrid framework, and integrating with DoE workflows, would further improve accuracy and interpretability.

Several limitations bound the interpretation of these results. The dataset is small (16 formulations) and derived from a single published source via digitization, so the bootstrap confidence intervals are wide and the numerical ranking among the leading models is not statistically distinguishable; the study is therefore best regarded as a controlled proof-of-concept. Hyperparameters were fixed a priori rather than systematically tuned, and the underfitting of SVR and GPR reflects this. The work concerns a single drug (glipizide) and three carriers, so quantitative transfer to other compounds or release mechanisms should not be assumed. There is no external or experimental validation. Finally, the largest errors occurred for unique reference formulations that are singletons under leave-one-formulation-out evaluation.

5. CONCLUSION

This study explored the efficacy of ML methods in predicting the complete in vitro dissolution profiles of glipizide SDs, leveraging both formulation and time-dependent information. A five-fold cross-validation approach was employed to minimize data leakage, ensuring that dissolution time points from the same formulation were not included in both the training and testing datasets, despite the limited size of the data. Among the models tested, bagged trees and LSTM sequence-to-sequence models exhibited the highest accuracy, with RMSEs of 18.90% and 19.18% and R^2 values of 0.701 and 0.692, respectively. The study highlighted that both nonlinear ensemble and sequential modeling methods effectively described the significant relationships between formulation, polymer, time, and drug release. Notably, bagged trees outperformed others, suggesting that ensemble decision-tree models can effectively capture complex, nonlinear dissolution-interactions with minimal data. The LSTM model demonstrated strong capability in modeling dissolution as a time-dependent sequence, capturing crucial temporal patterns in dissolution trajectories. Curve-level analysis confirmed that prominent models differentiated between polymer families and key dissolution characteristics, though some outliers arose under strict conditions. In contrast, SVR and GPR models showed inferior performance, including instances of constant predictions leading to negative R^2 values, likely due to the small number of independent formulations and limited dataset diversity. The results indicate the potential of ML, combined with traditional dissolution models, to create a data-driven approach for predicting release profiles, potentially reducing experimental efforts in the early stages of formulation development. However, conclusions are constrained by the limited dataset and the reliance on digital dissolution profiles from existing studies. Future research should involve larger, more diverse datasets encompassing raw dissolution measurements from various polymers and formulations. Validation through external experiments is also necessary to bolster the practical utility of these models for rapid screening and optimization of poorly soluble drug formulations.

ACKNOWLEDGMENTS

The authors thank Al-Ahliyya Amman University for institutional support.

FUNDING INFORMATION

Authors state no funding involved.

AUTHOR CONTRIBUTIONS STATEMENT

This journal uses the Contributor Roles Taxonomy (CRediT) to recognize individual author contributions, reduce authorship disputes, and facilitate collaboration.

Name of Author	C	M	So	Va	Fo	I	R	D	O	E	Vi	Su	P	Fu
Ali Olamat	✓	✓	✓	✓	✓	✓	✓	✓	✓	✓	✓	✓	✓	
Hamza Abu Owida	✓	✓	✓	✓	✓	✓	✓		✓	✓	✓	✓	✓	
Areen Arabiat		✓	✓	✓	✓	✓		✓	✓	✓	✓			
Pinar Ozel			✓	✓	✓					✓				

C : **C**onceptualization
M : **M**ethodology
So : **So**ftware
Va : **Va**lidation
Fo : **Fo**rmal analysis
I : **I**nvestigation
R : **R**esources
D : **D**ata Curation
O : Writing - **O**riginal Draft
E : Writing - Review & **E**diting
Vi : **Vi**sualization
Su : **Su**pervision
P : **P**roject administration
Fu : **Fu**nding acquisition

CONFLICT OF INTEREST STATEMENT

Authors state no conflict of interest.

DATA AVAILABILITY

The digitized dissolution dataset and all MATLAB analysis scripts are openly available at https://github.com/AliOlamat/Machine-Learning-Driven-Prediction-of-In-Vitro-Dissolution-Profiles-for-Glipizide-Solid-Dispersions. A permanent, citable snapshot will be archived via Zenodo upon acceptance. The underlying source curves are reproduced from [22].

REFERENCES

[1] M. Dumarey *et al.*, "Dissolution of Oral Solid Dosage Formulations: Surrogate Models and Real-time Release," *AAPS Journal*, vol. 27, no. 5, p. 115, Jun. 2025, doi: 10.1208/s12248-025-01102-0.

[2] T. R. Lex, J. D. Rodriguez, L. Zhang, W. Jiang, and Z. Gao, "Development of In Vitro Dissolution Testing Methods to Simulate Fed Conditions for Immediate Release Solid Oral Dosage Forms," *AAPS Journal*, vol. 24, no. 2, p. 40, Mar. 2022, doi: 10.1208/s12248-022-00690-5.

[3] Saudi Food and Drug Authority (SFDA), "Specifications: test procedures and acceptance criteria for new veterinary drug substances and new medicinal products: chemical substances (VICH GL39)," [Online]. Available: https://www.sfda.gov.sa/en/guide/specifications-test-procedures-and-acceptance-criteria-new-veterinary-drug-substances-and-new.

[4] N. Bouwhuis *et al.*, "Pharmacokinetic Cross-Over Study of Pharmacy-Compounded Chenodeoxycholic Acid Capsules Compared to Authorized Capsules," *Pharmaceutics*, vol. 17, no. 12, p. 1525, Nov. 2025, doi: 10.3390/pharmaceutics17121525.

[5] S. Liu, X. Cai, M. Shen, and Y. Tsong, "In vitro dissolution profile comparison using bootstrap bias corrected similarity factor, f2," *Journal of Biopharmaceutical Statistics*, vol. 34, no. 1, pp. 78–89, Jan. 2024, doi: 10.1080/10543406.2023.2171429.

[6] H. Malinowski *et al.*, "FDA guidance for industry extended release solid oral dosage forms: Development, evaluation, and application of in vitro/in vivo correlations," *Dissolution Technologies*, vol. 4, no. 4, pp. 23–32, 1997, doi: 10.14227/DT040497P23.

[7] A. Dokoumetzidis and P. Macheras, "A century of dissolution research: From Noyes and Whitney to the Biopharmaceutics Classification System," *International Journal of Pharmaceutics*, vol. 321, no. 1–2, pp. 1–11, Jul. 2006, doi: 10.1016/j.ijpharm.2006.07.011.

[8] A. A. Noyes and W. R. Whitney, "The rate of solution of solid substances in their own solutions," *Journal of the American Chemical Society*, vol. 19, no. 12, pp. 930–934, Dec. 1897, doi: 10.1021/ja02086a003.

[9] G. L. Amidon, H. Lennernäs, V. P. Shah, and J. R. Crison, "A Theoretical Basis for a Biopharmaceutic Drug Classification: The Correlation of in Vitro Drug Product Dissolution and in Vivo Bioavailability," *Pharmaceutical Research: An Official Journal of the American Association of Pharmaceutical Scientists*, vol. 12, no. 3, pp. 413–420, Mar. 1995, doi: 10.1023/A:1016212804288.

[10] C. Leuner and J. Dressman, "Improving drug solubility for oral delivery using solid dispersions," *European Journal of Pharmaceutics and Biopharmaceutics*, vol. 50, no. 1, pp. 47–60, Jul. 2000, doi: 10.1016/S0939-6411(00)00076-X.

[11] T. Vasconcelos, B. Sarmento, and P. Costa, "Solid dispersions as strategy to improve oral bioavailability of poor water soluble drugs," *Drug Discovery Today*, vol. 12, no. 23–24, pp. 1068–1075, Dec. 2007, doi: 10.1016/j.drudis.2007.09.005.

[12] W. L. Chiou, "Pharmaceutical applications of solid dispersion systems: X-ray diffraction and aqueous solubility studies on griseofulvin-polyethylene glycol 6000 systems," *Journal of Pharmaceutical Sciences*, vol. 66, no. 7, pp. 989–991, Jul. 1977, doi: 10.1002/jps.2600660722.

[13] K. Sekiguchi and N. Obi, "Studies on Absorption of Eutectic Mixture. I. A Comparison of the Behavior of Eutectic Mixture of Sulfathiazole and that of Ordinary Sulfathiazole in Man," *Chemical and Pharmaceutical Bulletin*, vol. 9, no. 11, pp. 866–872, 1961, doi: 10.1248/cpb.9.866.

[14] D. Q. M. Craig, "The mechanisms of drug release from solid dispersions in water-soluble polymers," *International Journal of Pharmaceutics*, vol. 231, no. 2, pp. 131–144, Jan. 2002, doi: 10.1016/S0378-5173(01)00891-2.

[15] S. Janssens and G. Van den Mooter, "Review: physical chemistry of solid dispersions," *Journal of Pharmacy and Pharmacology*, vol. 61, no. 12, pp. 1571–1586, Dec. 2009, doi: 10.1211/jpp.61.12.0001.

[16] P. Bannigan, M. Aldeghi, Z. Bao, F. Häse, A. Aspuru-Guzik, and C. Allen, "Machine learning directed drug formulation development," *Advanced Drug Delivery Reviews*, vol. 175, p. 113806, Aug. 2021, doi: 10.1016/j.addr.2021.05.016.

[17] Z. Bao, J. Bufton, R. J. Hickman, A. Aspuru-Guzik, P. Bannigan, and C. Allen, "Revolutionizing drug formulation development: The increasing impact of machine learning," *Advanced Drug Delivery Reviews*, vol. 202, p. 115108, Nov. 2023, doi: 10.1016/j.addr.2023.115108.

[18] C. Protopapa, A. Siamidi, A. A. Eneli, M. Elbadawi, and M. Vlachou, "Machine Learning Predicts Drug Release Profiles and Kinetic Parameters Based on Tablets' Formulations," *AAPS Journal*, vol. 27, no. 5, p. 124, Jul. 2025, doi: 10.1208/s12248-025-01101-1.

[19] A. S. Lourenço, T. Schuster, J. A. Lopes, and A. Kirsch, "A non-linear modelling approach to predict the dissolution profile of extended-release tablets," *European Journal of Pharmaceutical Sciences*, vol. 204, p. 106976, Jan. 2025, doi: 10.1016/j.ejps.2024.106976.

[20] M. Bharathi, R. Kamaraj, S. Murugaanandam, K. Navyaja, and T. S. Kumar, "A data-driven approach to predict the in vitro dissolution time of sustained-release tablets using raw material databases and machine learning algorithms," *Pharmacia*, vol. 71, pp. 1–7, Aug. 2024, doi: 10.3897/PHARMACIA.71.E122772.

[21] B. M. Castro *et al.*, "Machine learning predicts 3D printing performance of over 900 drug delivery systems," *Journal of Controlled Release*, vol. 337, pp. 530–545, Sep. 2021, doi: 10.1016/j.jconrel.2021.07.046.

[22] B. S. Alotaibi *et al.*, "Formulation and characterization of glipizide solid dosage form with enhanced solubility," *PLoS ONE*, vol. 19, no. 2 February, p. e0297467, Feb. 2024, doi: 10.1371/journal.pone.0297467.

[23] A. R. Smitha, J. Mohanan, A. K. Chalil, and F. N. Karakkunnummal, "Advances in Self-Nanoemulsifying Drug Delivery Systems: Mechanistic Insights and Formulation Strategies," *Journal of Drug Delivery and Therapeutics*, vol. 15, no. 8, pp. 217–236, Aug. 2025, doi: 10.22270/jddt.v15i8.7303.

[24] M. A. Kalam *et al.*, "Solubility Measurement and Various Solubility Parameters of Glipizide in Different Neat Solvents," *ACS Omega*, vol. 5, no. 3, pp. 1708–1716, Jan. 2020, doi: 10.1021/acsomega.9b04004.

[25] M. H. G. Dehghan, M. Saifee, and R. M. Hanwate, "Comparative Dissolution Study of Glipizide by Solid Dispersion Technique," *Journal of Pharmaceutical Science and Technology*, vol. 2, no. 9, pp. 293–297, 2010.

[26] H. Gao, W. Wang, J. Dong, Z. Ye, and D. Ouyang, "An integrated computational methodology with data-driven machine learning, molecular modeling and PBPK modeling to accelerate solid dispersion formulation design," *European Journal of Pharmaceutics and Biopharmaceutics*, vol. 158, pp. 336–346, Jan. 2021, doi: 10.1016/j.ejpb.2020.12.001.

[27] H. A. Owida, S. A. Hasan, A. Arabiat, and S. Abuowaida, "In Vitro liposome release profile prediction using explainable machine learning approaches," *PLOS One*, vol. 21, no. 8, p. e0354293, Aug. 2026, doi: 10.1371/journal.pone.0354293.

[28] M. Bansal, A. Goyal, and A. Choudhary, "A comparative analysis of K-Nearest Neighbor, Genetic, Support Vector Machine, Decision Tree, and Long Short Term Memory algorithms in machine learning," *Decision Analytics Journal*, vol. 3, p. 100071, May 2022, doi: 10.1016/j.dajour.2022.100071.

BIOGRAPHIES OF AUTHORS



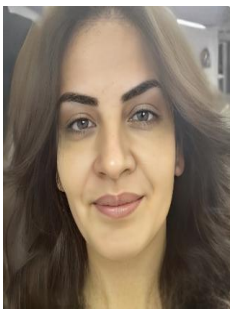
Ali Olamat assistant professor of Biomedical Engineering at Al-Ahliyya Amman University. His research interests include biomedical image processing, signal and systems, and AI-driven signal processing (AI DSP). He work on developing and applying computational methods to analyze biomedical data, extract meaningful features, and support improving diagnostics and decision-making in healthcare. He can be contacted at email: a.olamat@ammanu.edu.jo.



Hamza Abu Owida Ph.D. in biomedical engineering, associated professor at the Department of Medical Engineering, Al-Ahliyya Amman University, Jordan. Research interests focused on biomedical sensors, nanotechnology, and tissue engineering. He can be contacted at email: h.abuowida@ammanu.edu.jo.



Areen Arabiat earned her B.Sc. in Computer Engineering in 2009 from Aal Balqaa Applied University (BAU), and her M.Sc. in Intelligent Transportation Systems (ITS) from Al Ahliyya Amman University (AAU) in 2022. She is currently a computer lab supervisor, researcher and part-time lecturer in the Department of Communications and Computer Engineering at Al-Ahliyya Amman University since 2013. Her research interests are focused on the following areas: machine learning, data mining, image processing, internet of things (IoT), cyber security, wireless sensor network (WSN), artificial intelligence, and intelligent transportation system (ITS). She can be contacted at email: a.arabiat@ammanu.edu.jo.



Pinar Ozel is an academic and researcher specializing in biomedical engineering, signal processing, machine learning, deep learning, and brain-computer interfaces. She completed her Ph.D. in Biomedical Engineering at Istanbul University, following her M.Sc. in Biomedical Engineering at Boğaziçi University and her B.Sc. in Electrical and Electronics Engineering at Erciyes University. She also conducted postdoctoral research at the University of Tübingen, Germany. Her academic and research work focuses particularly on EEG signal analysis, emotion recognition, functional brain connectivity, multimedia learning, eye tracking, and neuroimaging applications. She can be contacted at email: pozell@gmail.com.